

# Theory of rotational linestrengths for resonant four-wave-mixing processes in gaseous media with application to CARS

Ilse Aben, Wim Ubachs, Gert van der Zwan and Wim Hogervorst

*Laser Centre Free University Amsterdam, De Boelelaan 1081, 1081 HV Amsterdam, The Netherlands*

Received 14 August 1992

The elements of the fourth rank non-linear susceptibility tensor  $\chi^{(3)}$  are considered for four-wave-mixing processes in a gaseous medium. In case of an isotropic medium 21 elements are non-zero, but only 3 are independent. Analytical expressions are derived for rotational linestrengths corresponding to these independent elements in multiple resonant four-wave mixing (FWM). These analytical expressions are appropriate for diatomic and symmetric-top molecules. The application of the model to resonant CARS processes observed in gaseous  $\text{Br}_2$  and  $\text{I}_2$  is illustrated. The effect of different polarization configurations of the incoming waves on the polarization of the generated anti-Stokes wave was investigated experimentally as well as theoretically for one of the resonant CARS processes in  $\text{I}_2$ . The rotational linestrength expressions have a general validity and may also be used in the case of non-saturated degenerate four-wave mixing.

## 1. Introduction

Over the last two decades coherent light scattering techniques have been developed into versatile tools for non-intrusive measurements in hostile environments. The method of coherent anti-Stokes Raman spectroscopy (CARS) is now commonly used for temperature and concentration measurements in the gas phase [1,2]. However for the detection of minor species, such as free radicals present as intermediates in combustion processes, the conventional CARS-technique is not suitable. Interference with non-resonant background signals hampers sensitive detection of diluted species. This drawback was overcome by using the complicated technique of three-color resonance-enhanced CARS [3]. Recently the analogous but experimentally simpler method of degenerate four-wave mixing (DFWM) [4–6] was introduced as a sensitive method for the detection of trace molecules in flames. For quantitative analysis of the recorded spectra in terms of temperatures and concentrations a theory for the calculation of rotational linestrengths in case of multiply resonant four-wave mixing (FWM) processes is required. Abrams and Lind [7] developed a theory for DFWM that is particularly applicable in cases of saturation. A theory of linestrengths based on an evaluation of the third order non-linear susceptibility  $\chi^{(3)}$  tensor, involving coherent sums over four-photon matrix elements was developed by Attal et al. [8] and by Aben et al. [9].

In this paper we present a formalism for the calculation of rotational linestrengths that is applicable to all possible combinations of polarizations of the incident and generated waves. Analytical expressions of rotational linestrengths are derived for the three independent  $\chi^{(3)}$  elements that describe threefold-resonant FWM in isotropic gaseous media. The elements of  $\chi^{(3)}$  are inspected for a variety of multiply resonant FWM processes in gaseous media including resonances on bound and continuum states.

Experimentally we investigated threefold-resonant FWM processes in isotropic  $\text{I}_2$  and  $\text{Br}_2$  vapours. For various types of resonant CARS processes the calculations of linestrengths were compared with observations and good agreement is found. Apart from the effects of arbitrary polarization orientations for the incident beams

*Correspondence to:* W. Ubachs, Laser Centre Free University Amsterdam, De Boelelaan 1081, 1081 HV Amsterdam, The Netherlands.

also the polarization of the generated wave was investigated. It is shown that in a particular geometrical setup the polarization of the anti-Stokes wave depends on the specific FWM process and the resonances involved.

The theory to calculate linestrengths is not restricted to the resonance CARS processes in diatomics such as  $I_2$  and  $Br_2$ , but also holds for various FWM processes in polyatomic symmetric-top molecules. Moreover it is capable of calculating linestrengths for DFWM processes as well.

## 2. Theoretical framework

### 2.1. Definition of the $\chi^{(3)}$ tensor

In a FWM process a wave is generated with frequency  $\omega = \pm\omega_1 \pm \omega_2 \pm \omega_3$  from incoming waves with frequencies  $\omega_1$ ,  $\omega_2$  and  $\omega_3$  respectively. The intensity of the generated FWM wave is proportional to the absolute square of the induced third-order non-linear polarization [10,11]:

$$I(\omega) \propto |P^{(3)}(\omega)|^2 = |\chi^{(3)}(\omega); E_{\omega_1} E_{\omega_2} E_{\omega_3}|^2, \quad (1)$$

in which  $\chi^{(3)}(\omega)$  is the third-order non-linear susceptibility tensor of rank four. The fields  $E_{\omega_i}$  represent monochromatic plane waves with frequencies  $\omega_i$ . The  $\chi^{(3)}$  tensor represents the characteristic response of the medium. The  $\chi^{(3)}$  elements are independent of the field components; however the polarizations of the fields determine which elements of  $\chi^{(3)}$  are needed to describe the FWM response. The Cartesian components of the non-linear induced polarization at  $\omega$  are given by

$$P_p^{(3)}(\omega) = \frac{1}{2^{n-1}} \sum_{\sigma, \tau, \nu} \chi_{p\sigma\tau\nu}^{(3)}(-\omega; \omega_1, \omega_2, \omega_3) (E_{\omega_1})_\sigma (E_{\omega_2})_\tau (E_{\omega_3})_\nu. \quad (2)$$

The ordering of the frequency terms and polarization indices ( $\sigma$ ,  $\tau$ ,  $\nu$ ) is arbitrary as long as the pairs ( $\sigma$ ,  $\omega_1$ ) etc. are considered together (see section 2.3).  $n$  is the number of incident frequencies. In the most general case  $n=3$ .

In FWM each one of the 81  $\chi_{p\sigma\tau\nu}^{(3)}$  tensor elements consists of 48 terms of the following form [12]:

$$\chi_{p\sigma\tau\nu}^{(3)}(-\omega; \omega_1, \omega_2, \omega_3) = N \sum_{a,b,c,d} \rho_{aa}^{(0)} \frac{\langle a | \mu_\sigma | b \rangle \langle b | \mu_\tau | c \rangle \langle c | \mu_\nu | d \rangle \langle d | \mu_p | a \rangle}{(\omega_{ba} - \omega_1 - i\Gamma_{ba})(\omega_{ca} - \omega_1 - \omega_2 - i\Gamma_{ca})(\omega_{da} - \omega - i\Gamma_{da})}. \quad (3)$$

Here  $|a\rangle$ ,  $|b\rangle$ ,  $|c\rangle$  and  $|d\rangle$  are rovibronic molecular states and  $\mu_\sigma$  is the component of the transition dipole moment vector in the laboratory frame along the Cartesian  $\sigma$  axis.  $\omega_{ij}$  is the transition frequency from state  $|i\rangle$  to  $|j\rangle$ . Resonances are damped by the relaxation parameter  $\Gamma_{ij}$ .  $\rho_{aa}^{(0)}$  represents the relative population distribution over initially populated states  $|a\rangle$  of the system. Only contributions from FWM processes probing a population density  $N\rho_{aa}^{(0)}$  in the electronic and vibrational ground state  $|a\rangle$  are considered.

In threefold-resonant CARS the intensity at a particular resonance in the spectrum is dominated by one or just a few terms in  $\chi^{(3)}$ . Moreover, at a specific wavelength combination only a few well-defined states  $|a\rangle$ ,  $|b\rangle$ ,  $|c\rangle$  and  $|d\rangle$  are involved [13]. At resonance the summation over all non-degenerate states then can be dropped. However, the summation over the degenerate  $M_J$  states has to be maintained. The three so-called resonance denominators of eq. (3) determine at which combinations of frequencies resonance-enhancement of FWM occurs in the medium. The rate of enhancement is then governed by the values of the three damping factors  $\Gamma_{ij}$ . In the present analysis it is assumed that for a specific FWM process the effect of the  $\Gamma$ 's is similar for all spectral components, i.e. independent of rotational quantum numbers. In that case the product of resonance denominators in  $\chi^{(3)}$  has a certain, but constant value and may be dropped from the considerations on rotational linestrengths. This leaves the following expression to be evaluated:

$$\chi_{\rho\sigma\tau\nu}^{(3)}(-\omega; \omega_1, \omega_2, \omega_3) \propto \sum_{M_a, M_b, M_c, M_d} \langle a | \mu_\sigma | b \rangle \langle b | \mu_\tau | c \rangle \langle c | \mu_\nu | d \rangle \langle d | \mu_\rho | a \rangle. \quad (4)$$

In a previous study [9] the procedure for further evaluation of this equation was described in detail. At this point we will summarize this procedure and discuss the implications of the results in a more general way.

## 2.2. Definition of the linestrength factors $S_{jklm}^{abcd}$

For a calculation of linestrengths in threefold-resonant FWM a coherent sum over the product of the four transition matrix elements of eq. (4) needs to be evaluated. Applying the Born–Oppenheimer approximation the wavefunction of state  $|a\rangle$  can be separated in an electronic, a vibrational and a rotational part:

$$|a\rangle = |\phi_a^{\text{electr.}}\rangle |\Phi_{\nu_a}^{\text{vib.}}\rangle |J_a \Omega_a M_a\rangle. \quad (5)$$

Here  $J$  is the total angular momentum,  $\Omega$  is its projection onto the internuclear axis and  $M$  is the projection of  $J$  on the space fixed  $z$  axis.  $\Omega$  also equals the projection of the electronic angular momentum onto the internuclear axis [14]. It should be noted that it is not straightforward to apply eq. (5) to all open-shell diatomic molecules. For diatomics in a singlet state the rotational part may be written as  $|J_a A_a M_a\rangle$  with  $A_a$  the projection of the electronic orbital angular momentum onto the internuclear axis; in this case all following derivations can be applied directly. This also holds for Hund's case (c) molecules that are commonly written in a  $|J_a \Omega_a M_a\rangle$  basis. In other cases, such as e.g. doublet states, more complicated wavefunctions must be invoked [8]. The corresponding quantum numbers in a symmetric top are  $J$ ,  $K$  and  $M$  respectively where  $K$  is the projection of  $J$  onto the symmetry axis and  $K = -J, -J+1, \dots, J$ . The set of  $K$  values is therefore usually much larger than that of  $\Omega$  values.

The dipole vector components in the space fixed frame ( $\mu_x, \mu_y, \mu_z$ ) are rewritten in spherical components ( $\mu_1, \mu_0, \mu_{-1}$ ). To characterize the system a transformation to the molecular frame using Euler angles ( $\alpha, \beta, \gamma$ ) is required. The dipole transition matrix elements between arbitrary states  $|a\rangle$  and  $|b\rangle$  may then be factorized in terms of a pure electronic dipole transition matrix element, a vibrational overlap factor and a rotational part that depends on the polarization components of the light:

$$\begin{aligned} \langle J_a \Omega_a M_a | \mu_\sigma | J_b \Omega_b M_b \rangle &= \sum_{m, m'} (-1)^{m'} e_{-m}^\sigma \mu_{ab}^{\Omega_a - \Omega_b} F_{ab} \sqrt{\frac{2J_b + 1}{2J_a + 1}} \delta_{M_a - m - M_b, 0} \delta_{\Omega_a - m' - \Omega_b, 0} \\ &\times \langle J_b, -M_b, 1, -m | J_a, -M_b - m \rangle \langle J_b, -\Omega_b, 1, -m' | J_a, -\Omega_b - m' \rangle. \end{aligned} \quad (6)$$

Here the last two factors written in brackets denote Clebsch–Gordan coefficients in the notation of Zare [14]. The vibrational overlap factor is denoted by  $F_{ab}$ ,  $\mu_{ab}^{\Omega_a - \Omega_b}$  is the electronic transition matrix element and  $e_{-m}^\sigma$  denotes the projection of the Cartesian  $\sigma$  axis on the spherical  $m$  axis. Evaluation of the product of four dipole transition matrix elements, each written in the form of eq. (6) and inserted in eq. (4), then yields a product of four electronic dipole transition moments, four vibrational overlap factors and a rotational linestrength factor denoted by  $S_{jklm}^{abcd}$ . Consequently the third-order non-linear susceptibility depends on this linestrength factor in the following way:

$$\chi_{\rho\sigma\tau\nu}^{(3)}(-\omega; \omega_1, \omega_2, \omega_3) \propto \mu_{ab}^{\Omega_a - \Omega_b} \mu_{bc}^{\Omega_b - \Omega_c} \mu_{cd}^{\Omega_c - \Omega_d} \mu_{da}^{\Omega_d - \Omega_a} F_{ab} F_{bc} F_{cd} F_{da} \sum_{j, k, l, m} e_{-j}^\sigma e_{-k}^\tau e_{-l}^\nu e_{-m}^\rho S_{jklm}^{abcd}. \quad (7)$$

By careful bookkeeping and summing over Clebsch–Gordan coefficients [9] an expression for the rotational linestrength factor follows:

$$S_{jklm}^{abcd} = \Omega^{abcd} S_{jklm}. \quad (8a)$$

Here  $\Omega^{abcd}$  is the molecular prefactor:

$$\Omega^{abcd} = \langle J_b, -\Omega_b, 1, \Omega_b - \Omega_a | J_a, -\Omega_a \rangle \langle J_c, -\Omega_c, 1, \Omega_c - \Omega_b | J_b, -\Omega_b \rangle$$

$$\times \langle J_d, -\Omega_d, 1, \Omega_d - \Omega_c | J_c, -\Omega_c \rangle \langle J_a, -\Omega_a, 1, \Omega_a - \Omega_d | J_d, -\Omega_d \rangle, \quad (8b)$$

and  $s_{jklm}$  the reduced linestrength factor:

$$S_{jklm} = \sum_{M_a} \delta_{j+k+l+m,0} f(M_a) \langle J_b, j-M_a, 1, -j | J_a, -M_a \rangle \langle J_c, k+j-M_a, 1, -k | J_b, j-M_a \rangle$$

$$\times \langle J_d, l+k+j-M_a, 1, -l | J_c, j+k-M_a \rangle \langle J_a, -M_a, 1, -m | J_d, j+k+l-M_a \rangle. \quad (8c)$$

The superscripts in  $S_{jklm}^{abcd}$  denote the electronic orbital momentum of states  $|a\rangle$ ,  $|b\rangle$ ,  $|c\rangle$  and  $|d\rangle$ , while the subscripts  $j$ ,  $k$ ,  $l$  and  $m$  represent the spherical components related to the Cartesian components  $\sigma$ ,  $\tau$ ,  $\nu$  and  $\rho$  of the polarization of the light. Whenever the superscripts are not important they are left out of the notation. The molecular prefactor  $\Omega^{abcd}$  depends only on the specific electronic angular momenta of the states involved ( $\Omega_a$ ,  $\Omega_b$ ,  $\Omega_c$ ,  $\Omega_d$ ) and can easily be calculated. The reduced linestrength factor  $s_{jklm}$  depends on the polarization configuration through  $j$ ,  $k$ ,  $l$  and  $m$  and involves a summation over degenerate  $M_a$  values. The summation over  $M_a$  states is weighted by a function  $f(M_a)$  to account for possible non-isotropic distributions of  $\mathbf{J}$  vectors. We note that the reduced linestrength factor is independent of the sequences of electronic angular momenta and may therefore be calculated independent of the particular electronic resonances involved in the FWM process. However, both the molecular prefactor and the reduced linestrength factor depend on the specific ( $J_a$ ,  $J_b$ ,  $J_c$ ,  $J_d$ ) combination involved.

The relation between elements of the non-linear susceptibility tensor and the rotational linestrength factors is determined by the transformation from Cartesian into spherical coordinates given by eq. (7). It follows that a Cartesian component of the  $\chi^{(3)}$  susceptibility tensor involves in principle a sum over spherical linestrength factors  $S$ .

The relation between the  $\chi^{(3)}$  elements and the  $S$  factors also depends on the resonance scheme of the particular FWM process. The schemes that we consider here are shown in fig. 1 and are all of the type  $\omega_{AS} = 2\omega_1 - \omega_2$ . The elements of the tensor  $\chi_{\rho\sigma\tau\nu}^{(3)}$  are determined by eq. (2):

$$\chi_{\rho\sigma\tau\nu}^{(3)I}(-\omega_{AS}; \omega_1, \omega_1, -\omega_2) \propto \langle a | \mu_\sigma | b \rangle \langle b | \mu_\nu | c \rangle \langle c | \mu_\tau | d \rangle \langle d | \mu_\rho | a \rangle + (\sigma \leftrightarrow \tau),$$

$$\chi_{\rho\sigma\tau\nu}^{(3)II}(-\omega_{AS}; \omega_1, \omega_1, -\omega_2) \propto \langle a' | \mu_\sigma | b' \rangle \langle b' | \mu_\tau | c' \rangle \langle c' | \mu_\nu | d' \rangle \langle d' | \mu_\rho | a' \rangle + (\sigma \leftrightarrow \tau),$$

$$\chi_{\rho\sigma\tau\nu}^{(3)III}(-\omega_{AS}; \omega_1, \omega_1, -\omega_2) \propto \langle a'' | \mu_\sigma | b'' \rangle \langle b'' | \mu_\tau | c'' \rangle \langle c'' | \mu_\rho | d'' \rangle \langle d'' | \mu_\nu | a'' \rangle + (\sigma \leftrightarrow \tau), \quad (9)$$

where the subscripts I, II and III refer to the resonance schemes of fig. 1. Due to the degeneracy in the  $\omega_1$  field the  $\chi_{\rho\sigma\tau\nu}^{(3)}$  element contains two terms which are nearly identical except for the permutation ( $\sigma \leftrightarrow \tau$ ). As an example we express the  $\chi_{xzxx}^{(3)}$  element in the corresponding linestrength factors. For the ground state CARS process of fig. 1 we get

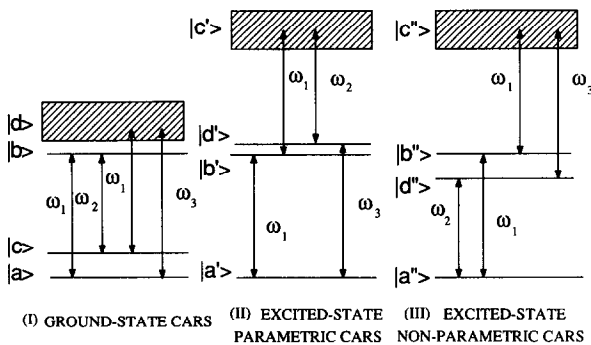


Fig. 1. Energy level diagrams corresponding to ground-state CARS, excited-state parametric CARS and excited-state non-parametric CARS.

$$\begin{aligned} \chi_{zzzz}^{(3)} &\propto \sum_{j,k,l,m} e^{\sigma_j} e^{\nu_k} e^{\tau_l} e^{\rho_m} S_{jklm} + \sum_{j,k,l,m} e^{\tau_j} e^{\nu_k} e^{\sigma_l} e^{\rho_m} S_{jklm} \\ &= -\frac{1}{2}(-S_{0101} - S_{0-10-1} + S_{010-1} + S_{0-101}) - \frac{1}{2}(-S_{0101} - S_{0-10-1} + S_{010-1} + S_{0-101}) = -2S_{10-10}, \end{aligned} \quad (10)$$

where use is made of some symmetry properties of the  $S_{jklm}$  elements pertaining to an *isotropic* medium to be discussed in the next section. In the case of the other two FWM processes of fig. 1 other  $S_{jklm}$  elements must be evaluated which, however, correspond to the same element  $\chi_{zzzz}^{(3)}$ . The difference stems from the fact that the incoming polarized waves enter  $\chi^{(3)}$  at different resonances, which correspond to different transition matrix elements.

In the case of four parallel fields the evaluation of  $S_{0000}$  is needed independent of the particular FWM scheme. In the case of crossed polarizations of incident beams in the FWM processes of ground-state CARS (I), parametric excited-state CARS (II) and non-parametric excited-state CARS (III) (fig. 1) in an isotropic medium the elements  $S_{10-10}$ ,  $S_{1-100}$  and again  $S_{1-100}$  govern the rotational linestrengths (see section 3).

### 2.3. Symmetry considerations

The rotational linestrength factors  $S_{jklm}^{abcd}$  represent FWM processes, which imposes restrictions on the allowed combinations of  $j$ ,  $k$ ,  $l$  and  $m$ . The  $\delta_{j+k+l+m,0}$  function in eq. (8c) implies angular momentum conservation associated with the four-photon process [15]. Only 19 different ways of combining four (0,  $\pm 1$ ) values are possible, so 19 independent  $S$  elements differ from zero. The molecular prefactor in eq. (8b) connecting  $s$  to  $S$  is independent of  $j$ ,  $k$ ,  $l$ ,  $m$  and  $M_a$ . It can therefore be left out of the symmetry considerations.

The *macroscopic* symmetry of the medium enters into the equation through the weighted sum over  $M_a$  states in eq. (8c). Two cases will be considered: (1) a symmetrically aligned system where  $f(M_a) = f(-M_a)$  and (2) an isotropic system  $f(M_a) = 1$  for all  $M_a$  values. For both systems additional symmetry rules for the  $\chi^{(3)}$  elements can be derived through inspection of the linestrength factors in which they may be expressed.

The product of four Clebsch–Gordan coefficients in eq. (8c) is invariant for a change of  $j$ ,  $k$ ,  $l$ ,  $m$  and  $M_a$  into  $-j$ ,  $-k$ ,  $-l$ ,  $-m$  and  $-M_a$ . In the case of  $f(M_a) = f(-M_a)$  this yields 9 additional relations between the non-zero  $S$  elements leaving only 10 independent  $S$  elements.

In the case of an isotropic macroscopic ensemble with  $f(M_a) = 1$  for all  $M_a$  states extra symmetry relations apply:

$$\begin{aligned} S_{0000} &= -S_{100-1} - S_{1-100} - S_{10-10}, \\ -S_{001-1} &= -S_{1-100} = +\frac{1}{2}S_{1-1-11} + \frac{1}{2}S_{1-11-1} - \frac{1}{2}S_{11-1-1}, \\ -S_{010-1} &= -S_{10-10} = +\frac{1}{2}S_{1-1-11} - \frac{1}{2}S_{1-11-1} + \frac{1}{2}S_{11-1-1}, \\ -S_{-1001} &= -S_{100-1} = -\frac{1}{2}S_{1-1-11} + \frac{1}{2}S_{1-11-1} + \frac{1}{2}S_{11-1-1}. \end{aligned} \quad (11)$$

In Cartesian components this results in

$$\begin{aligned} \chi_{xxxx}^{(3)} = \chi_{yyyy}^{(3)} = \chi_{zzzz}^{(3)} &= \chi_{xyyx}^{(3)} + \chi_{xyxy}^{(3)} + \chi_{xxyy}^{(3)}, & \chi_{xxzz}^{(3)} = \chi_{yyzz}^{(3)} = \chi_{xxyy}^{(3)} = \chi_{yyxx}^{(3)} = \chi_{zzxx}^{(3)} = \chi_{zzyy}^{(3)}, \\ \chi_{zzxx}^{(3)} = \chi_{zyzy}^{(3)} = \chi_{xyxy}^{(3)} &= \chi_{yxxy}^{(3)} = \chi_{xzxz}^{(3)} = \chi_{yzyz}^{(3)}, & \chi_{xzzx}^{(3)} = \chi_{yzyy}^{(3)} = \chi_{xyyx}^{(3)} = \chi_{yxxy}^{(3)} = \chi_{zzxx}^{(3)} = \chi_{zyyz}^{(3)}. \end{aligned} \quad (12)$$

So for an isotropic ensemble there are 21  $\chi^{(3)}$  elements different from zero, with just 3 of them independent, namely  $\chi_{1122}^{(3)}$ ,  $\chi_{1212}^{(3)}$  and  $\chi_{1221}^{(3)}$  (with 1, 2 =  $x$ ,  $y$  or  $z$ ). This is consistent with the fact that for a fourth-rank tensor there are only three invariant elements under any operation of the point group representing an isotropic system.

Butcher [15] has shown that as a consequence of time reversal symmetry an intrinsic permutation symmetry of  $\chi^{(3)}$  holds for the pairs  $(\sigma, \omega_1)$ ,  $(\tau, \omega_2)$  and  $(\nu, \omega_3)$  in eq. (2). In the case of degenerate fields the intrinsic permutation symmetry results in additional relations between the  $\chi^{(3)}$  elements. For example in the case of

Table 1  
 Reduced rotational linestrength factors  $S_{jklm}$  (eq. (8c)) calculated for an isotropic distribution of  $J$  vectors in a gaseous medium

	$S_{0000}$	$S_{10-10}$
$[J, J-1, J-1, J]$	$-\frac{\sqrt{J-1}\sqrt{J+1}\sqrt{2J-1}\sqrt{2J+1}}{15J}$	$\frac{2\sqrt{J-1}\sqrt{J+1}\sqrt{2J-1}\sqrt{2J+1}}{15J}$
$[J, J+1, J, J]$	$-\frac{(J+2)\sqrt{2J+1}\sqrt{2J+3}}{15(J+1)}$	$-\frac{(J-3)\sqrt{2J+1}\sqrt{2J+3}}{30(J+1)}$
$[J, J, J+1, J+1]$	$-\frac{\sqrt{J}\sqrt{J+2}\sqrt{2J+1}\sqrt{2J+3}}{15(J+1)}$	$\frac{2\sqrt{J}\sqrt{J+2}\sqrt{2J+1}\sqrt{2J+3}}{15(J+1)}$
$[J, J, J+1, J]$	$-\frac{(J+2)\sqrt{2J+1}\sqrt{2J+3}}{15(J+1)}$	$-\frac{(J-3)\sqrt{2J+1}\sqrt{2J+3}}{30(J+1)}$
$[J, J, J, J+1]$	$-\frac{(J+2)\sqrt{2J+1}\sqrt{2J+3}}{15(J+1)}$	$-\frac{(J-3)\sqrt{2J+1}\sqrt{2J+3}}{30(J+1)}$
$[J, J, J, J-1]$	$-\frac{(J-1)\sqrt{2J-1}\sqrt{2J+1}}{15J}$	$-\frac{(J+4)\sqrt{2J-1}\sqrt{2J+1}}{30J}$
$[J, J, J-1, J-1]$	$-\frac{\sqrt{J-1}\sqrt{J+1}\sqrt{2J-1}\sqrt{2J+1}}{15J}$	$\frac{2\sqrt{J-1}\sqrt{J+1}\sqrt{2J-1}\sqrt{2J+1}}{15J}$
$[J, J, J-1, J]$	$-\frac{(J-1)\sqrt{2J-1}\sqrt{2J+1}}{15J}$	$-\frac{(J+4)\sqrt{2J-1}\sqrt{2J+1}}{30J}$
$[J, J+1, J+1, J+1]$	$-\frac{J\sqrt{2J+1}\sqrt{2J+3}}{15(J+1)}$	$-\frac{(J+5)\sqrt{2J+1}\sqrt{2J+3}}{30(J+1)}$
$[J, J+1, J+1, J]$	$-\frac{\sqrt{J}\sqrt{J+2}\sqrt{2J+1}\sqrt{2J+3}}{15(J+1)}$	$\frac{2\sqrt{J}\sqrt{J+2}\sqrt{2J+1}\sqrt{2J+3}}{15(J+1)}$
$[J, J+1, J+2, J+1]$	$\frac{2\sqrt{2J+1}\sqrt{2J+5}}{15}$	$-\frac{\sqrt{2J+1}\sqrt{2J+5}}{10}$
$[J, J+1, J, J+1]$	$\frac{5+8J+4J^2}{15(J+1)}$	$\frac{2J(J+2)}{15(J+1)}$
$[J, J+1, J, J-1]$	$\frac{2\sqrt{2J-1}\sqrt{2J+3}}{15}$	$-\frac{\sqrt{2J-1}\sqrt{2J+3}}{10}$
$[J, J-1, J, J+1]$	$\frac{2\sqrt{2J-1}\sqrt{2J+3}}{15}$	$-\frac{\sqrt{2J-1}\sqrt{2J+3}}{10}$
$[J, J-1, J, J-1]$	$\frac{4J^2+1}{15J}$	$\frac{2(J-1)(J+1)}{15J}$
$[J, J-1, J-1, J-1]$	$-\frac{(J+1)\sqrt{2J-1}\sqrt{2J+1}}{15J}$	$-\frac{(J-4)\sqrt{2J-1}\sqrt{2J+1}}{30J}$
$[J, J-1, J-2, J-1]$	$\frac{2\sqrt{2J+1}\sqrt{2J-3}}{15}$	$-\frac{\sqrt{2J+1}\sqrt{2J-3}}{10}$
$[J, J, J, J]$	$\frac{6J^3+9J^2+J-1}{15J(J+1)}$	$-\frac{(J-1)(J+2)(2J+1)}{15J(J+1)}$
$[J, J-1, J, J]$	$-\frac{(J-1)\sqrt{2J-1}\sqrt{2J+1}}{15J}$	$-\frac{(J+4)\sqrt{2J-1}\sqrt{2J+1}}{30J}$

Table 1  
(Continued)

	$S_{1-100}$	$S_{100-1}$
$[J, J-1, J-1, J]$	$\frac{-\sqrt{J-1}\sqrt{J+1}\sqrt{2J-1}\sqrt{2J+1}}{30J}$	$\frac{-\sqrt{J-1}\sqrt{J+1}\sqrt{2J-1}\sqrt{2J+1}}{30J}$
$[J, J+1, J, J]$	$\frac{(4J+3)\sqrt{2J+1}\sqrt{2J+3}}{30(J+1)}$	$\frac{-(J+2)\sqrt{2J+1}\sqrt{2J+3}}{30(J+1)}$
$[J, J, J+1, J+1]$	$\frac{-\sqrt{J}\sqrt{J+2}\sqrt{2J+1}\sqrt{2J+3}}{30(J+1)}$	$\frac{-\sqrt{J}\sqrt{J+2}\sqrt{2J+1}\sqrt{2J+3}}{30(J+1)}$
$[J, J, J+1, J]$	$\frac{-(J+2)\sqrt{2J+1}\sqrt{2J+3}}{30(J+1)}$	$\frac{(4J+3)\sqrt{2J+1}\sqrt{2J+3}}{30(J+1)}$
$[J, J, J, J+1]$	$\frac{(4J+3)\sqrt{2J+1}\sqrt{2J+3}}{30(J+1)}$	$\frac{-(J+2)\sqrt{2J+1}\sqrt{2J+3}}{30(J+1)}$
$[J, J, J, J-1]$	$\frac{(4J+1)\sqrt{2J-1}\sqrt{2J+1}}{30J}$	$\frac{-(J-1)\sqrt{2J-1}\sqrt{2J+1}}{30J}$
$[J, J, J-1, J-1]$	$\frac{-\sqrt{J-1}\sqrt{J+1}\sqrt{2J-1}\sqrt{2J+1}}{30J}$	$\frac{-\sqrt{J-1}\sqrt{J+1}\sqrt{2J-1}\sqrt{2J+1}}{30J}$
$[J, J, J-1, J]$	$\frac{-(J-1)\sqrt{2J-1}\sqrt{2J+1}}{30J}$	$\frac{(4J+1)\sqrt{2J-1}\sqrt{2J+1}}{30J}$
$[J, J+1, J+1, J+1]$	$\frac{-J\sqrt{2J+1}\sqrt{2J+3}}{30(J+1)}$	$\frac{(4J+5)\sqrt{2J+1}\sqrt{2J+3}}{30(J+1)}$
$[J, J+1, J+1, J]$	$\frac{-\sqrt{J}\sqrt{J+2}\sqrt{2J+1}\sqrt{2J+3}}{30(J+1)}$	$\frac{-\sqrt{J}\sqrt{J+2}\sqrt{2J+1}\sqrt{2J+3}}{30(J+1)}$
$[J, J+1, J+2, J+1]$	$\frac{\sqrt{2J+1}\sqrt{2J+5}}{15}$	$\frac{-\sqrt{2J+1}\sqrt{2J+5}}{10}$
$[J, J+1, J, J+1]$	$\frac{-(J+2)(6J+5)}{30(J+1)}$	$\frac{-J(6J+7)}{30(J+1)}$
$[J, J+1, J, J-1]$	$\frac{-\sqrt{2J-1}\sqrt{2J+3}}{10}$	$\frac{\sqrt{2J-1}\sqrt{2J+3}}{15}$
$[J, J-1, J, J+1]$	$\frac{-\sqrt{2J-1}\sqrt{2J+3}}{10}$	$\frac{-\sqrt{2J-1}\sqrt{2J+3}}{15}$
$[J, J-1, J, J-1]$	$\frac{-(J-1)(6J+1)}{30J}$	$\frac{-6J^2-5J+1}{30J}$
$[J, J-1, J-1, J-1]$	$\frac{-(J+1)\sqrt{2J-1}\sqrt{2J+1}}{30J}$	$\frac{(4J-1)\sqrt{2J-1}\sqrt{2J+1}}{30J}$
$[J, J-1, J-2, J-1]$	$\frac{\sqrt{2J+1}\sqrt{2J-3}}{15}$	$\frac{-\sqrt{2J+1}\sqrt{2J-3}}{10}$
$[J, J, J, J]$	$\frac{-(2J+1)(2J^2+2J+1)}{30J(J+1)}$	$\frac{-(2J+1)(2J^2+2J+1)}{30J(J+1)}$
$[J, J-1, J, J]$	$\frac{(4J+1)\sqrt{2J-1}\sqrt{2J+1}}{30J}$	$\frac{-(J-1)\sqrt{2J-1}\sqrt{2J+1}}{30J}$

CARS where two beams with frequencies  $\omega_1$  and  $\omega_2$  are used to generate a wave with frequency  $2\omega_1 - \omega_2$  the elements  $\chi_{1212}^{(3)}(-\omega; \omega_1, \omega_1, -\omega_2)$  are equal to  $\chi_{1122}^{(3)}(-\omega; \omega_1, \omega_1, -\omega_2)$  (with 1, 2 = x, y and z). So in an isotropic medium there are then only two independent  $\chi^{(3)}$  elements left namely  $\chi_{1212}^{(3)}(-\omega; \omega_1, \omega_1, -\omega_2)$  and  $\chi_{2211}^{(3)}(-\omega; \omega_1, \omega_1, -\omega_2)$ . For the case of ground state CARS for example the elements  $\chi_{1212}^{(3)}$  and  $\chi_{1122}^{(3)}$  equal  $(-S_{1-100} - S_{100-1})$  and  $(-S_{100-1} - S_{1-100})$  respectively. This is the justification for the inclusion of the ( $\sigma \leftrightarrow \tau$ ) factors in eq. (9) to account for the degeneracy in the  $\omega_1$  beams.

Overall permutation symmetry, or Kleinman symmetry [16], applies when the  $\chi^{(3)}$  elements are independent of the frequencies involved, so when the frequencies of the incoming fields which appear in the denominators of  $\chi^{(3)}$  are far removed from molecular transition frequencies. In that case all permutations of the subindices of the  $\chi^{(3)}$  tensor leave the elements unchanged and only a single independent tensor element remains. For the case of the threefold resonance-enhanced CARS processes described in this paper Kleinman symmetry obviously does not hold. For ground state CARS for example the elements  $\chi_{1212}^{(3)}$  and  $\chi_{2211}^{(3)}$  are equal to  $(-S_{1-100} - S_{100-1})$  and  $(-2S_{10-10})$  respectively. Table 1 shows that these elements are different.

## 2.4. Calculation of rotational linestrength factors $S$

### 2.4.1. Calculation of the reduced linestrength factors $s_{jklm}$

Now we return to an evaluation of the individual  $s_{jklm}$  factors. A sequence of four transition matrix elements, going from state  $|a\rangle$  through  $|b\rangle$ ,  $|c\rangle$  and  $|d\rangle$  back to  $|a\rangle$ , needs to be evaluated. For the transition matrix elements the general  $\Delta J = 0, \pm 1$  selection rule holds, therefore 19 different ( $J_a, J_b, J_c, J_d$ ) routes are allowed in general. This is illustrated in fig. 2.

The procedure to derive reduced  $s$  factors is elaborate because of the required summation over degenerate  $M_a$  values, appropriately weighted to account for possible macroscopic symmetry in the ensemble of molecules. The weighted summation over  $M_a$  states, ranging from  $-J_a$  to  $J_a$ , can always be performed numerically, but in some cases analytical expressions can be derived.

In the case of an isotropic medium there are three independent  $s$  factors ( $s_{10-10}$ ,  $s_{1-100}$  and  $s_{100-1}$ ). For all possible 19  $J$ -routes the summation over  $M_a$  for these 3 elements have been performed. The results are listed in table 1. The  $s_{0000}$  component is also given as it is needed in the case of linear and parallel polarizations of the incident waves.  $s_{0000}$  can also be obtained by adding the three independent components, in agreement with eq. (11).

### 2.4.2. Molecular prefactors $\Omega^{abcd}$

The molecular prefactors  $\Omega^{abcd}$  in the expressions for the rotational linestrength, defined by eq. (8b), are a simple product of four Clebsch–Gordan coefficients and involve only the total angular momentum  $J$  and the projection of the electronic angular momentum onto the internuclear axis of the molecule  $\Omega$ . In table 2 molecular

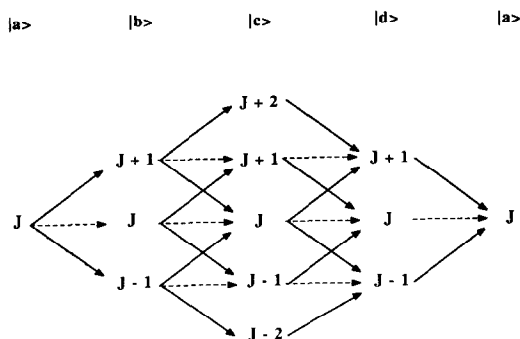


Fig. 2. Diagrammatic representation of  $J$  state sequences involved in a [ $J_a, J_b, J_c, J_d$ ] FWM cycle. The dashed one-photon interactions are forbidden when the two electronic states involved both have  $\Omega=0$  symmetry.

Table 2

Molecular prefactors  $\Omega^{abcd}$  (eq. (8b)) calculated for sequences of electronic states with  $\Omega_a = \Omega_b = \Omega_c = 0$ , or  $\pm 1$  and  $\Omega_d = 0$ , or  $\pm 1$ 

	$\Omega^{0000}$	$\Omega^{000\pm 1}$	$\Omega^{00\pm 10}$
$[J, J+1, J, J+1]$	$\frac{(J+1)(J+1)}{(2J+1)(2J+3)}$	$\frac{-(J+1)(J+2)}{2(2J+1)(2J+3)}$	$\frac{-J(J+1)}{2(2J+1)(2J+3)}$
$[J, J+1, J, J-1]$	$\frac{J(J+1)}{(2J+1)\sqrt{2J-1}\sqrt{2J+3}}$	$\frac{-(J-1)(J+1)}{2(2J+1)\sqrt{2J-1}\sqrt{2J+3}}$	$\frac{J(J+1)}{2(2J+1)\sqrt{2J-1}\sqrt{2J+3}}$
$[J, J+1, J, J]$	0	$\frac{(J+1)}{2\sqrt{2J+1}\sqrt{2J+3}}$	0
$[J, J+1, J+1, J+1]$	0	0	$\frac{(J+1)}{2\sqrt{2J+1}\sqrt{2J+3}}$
$[J, J+1, J+2, J+1]$	$\frac{(J+1)(J+2)}{(2J+3)\sqrt{2J+1}\sqrt{2J+5}}$	$\frac{(J+1)(J+2)}{2(2J+3)\sqrt{2J+1}\sqrt{2J+5}}$	$\frac{-(J+1)(J+3)}{2(2J+3)\sqrt{2J+1}\sqrt{2J+5}}$
$[J, J-1, J, J-1]$	$\frac{J^2}{(2J-1)(2J+1)}$	$\frac{-J(J-1)}{2(2J-1)(2J+1)}$	$\frac{-J(J+1)}{2(2J-1)(2J+1)}$
$[J, J-1, J, J+1]$	$\frac{J(J+1)}{(2J+1)\sqrt{2J-1}\sqrt{2J+3}}$	$\frac{-J(J+2)}{2(2J+1)\sqrt{2J-1}\sqrt{2J+3}}$	$\frac{J(J+1)}{2(2J+1)\sqrt{2J-1}\sqrt{2J+3}}$
$[J, J-1, J, J]$	0	$\frac{J}{2\sqrt{2J+1}\sqrt{2J-1}}$	0
$[J, J-1, J-1, J-1]$	0	0	$\frac{J}{2\sqrt{2J-1}\sqrt{2J+1}}$
$[J, J-1, J-2, J-1]$	$\frac{J(J-1)}{(2J-1)\sqrt{2J-3}\sqrt{2J+1}}$	$\frac{J(J-1)}{2\sqrt{2J+1}\sqrt{2J-1}}$	$\frac{-J(J-2)}{2(2J-1)\sqrt{2J+1}\sqrt{2J-3}}$

prefactors  $\Omega^{0000}$ ,  $\Omega^{000\pm 1}$  and  $\Omega^{00\pm 10}$  that play a role in the resonance CARS processes of fig. 1 in  $I_2$  and  $Br_2$  for all possible  $J$ -routes are given. In some interactions  $\Delta\Omega=0$  and Q branches are forbidden under this condition. In this case the number of possible pathways is smaller than 19. The extension of the present work to symmetric-top molecules requires elaborate calculations because the  $K$  value, representing the projection of the angular momentum on a molecule-fixed axis may range from  $-J$  to  $J$  and  $J$  may be a large number. The advantage of the present analysis is that the  $K$  value only appears in the molecular prefactors which are easily evaluated.

#### 2.4.3. Rotational linestrength factors $S_{jklm}^{abcd}$

Expressions for rotational linestrength factors  $S_{jklm}^{abcd}$  are obtained for each of the 19  $J$ -routes by multiplication of the appropriate molecular prefactor  $\Omega^{abcd}$  with the reduced linestrength factor  $S_{jklm}$ . We calculated the rotational linestrength factors for a sequence of four states with  $\Omega=0$ , with relevance for the resonance CARS experiments in  $I_2$  and  $Br_2$ . The four elements  $S_{0000}^{0000}$ ,  $S_{10-10}^{0000}$ ,  $S_{1-100}^{0000}$  and  $S_{100-1}^{0000}$ , given in table 3, govern the linestrengths in resonance CARS processes with arbitrary polarizations of the incident waves. Because  $\Omega=0$  for all electronic states involved only 6 different  $J$ -routes are allowed. In section 3 we will discuss the particular  $S$  factors that describe the so-called ground-state CARS spectra in  $Br_2$  and the excited state CARS spectra in  $I_2$  (see fig. 1).

Table 3  
Rotational line strength factors  $S_{klm}^{0000}$  (eq. (8a)) for  $\Omega_a = \Omega_b = \Omega_c = \Omega_d = 0$

	$S_{0000}^{0000}$	$S_{10-10}^{0000}$	$S_{1-100}^{0000}$	$S_{100-1}^{0000}$
$[J, J+1, J, J+1]$	$\frac{(J+1)(5+8J+4J^2)}{15(2J+1)(2J+3)}$	$\frac{2J(J+1)(J+2)}{15(2J+1)(2J+3)}$	$\frac{-(J+2)(6J+5)(J+1)}{30(2J+1)(2J+3)}$	$\frac{-J(J+1)(6J+7)}{30(2J+1)(2J+3)}$
$[J, J+1, J, J-1]$	$\frac{2J(J+1)}{15(2J+1)}$	$\frac{-J(J+1)}{10(2J+1)}$	$\frac{-J(J+1)}{10(2J+1)}$	$\frac{J(J+1)}{15(2J+1)}$
$[J, J+1, J+2, J+1]$	$\frac{2(J+1)(J+2)}{15(2J+3)}$	$\frac{-(J+1)(J+2)}{10(2J+3)}$	$\frac{(J+1)(J+2)}{15(2J+3)}$	$\frac{-(J+1)(J+2)}{10(2J+3)}$
$[J, J-1, J, J-1]$	$\frac{J(4J^2+1)}{15(2J-1)(2J+1)}$	$\frac{2J(J-1)(J+1)}{15(2J-1)(2J+1)}$	$\frac{-J(J-1)(6J+1)}{30(2J-1)(2J+1)}$	$\frac{J(-6J^2-5J+1)}{30(2J-1)(2J+1)}$
$[J, J-1, J, J+1]$	$\frac{2J(J+1)}{15(2J+1)}$	$\frac{-J(J+1)}{10(2J+1)}$	$\frac{-J(J+1)}{10(2J+1)}$	$\frac{-J(J+1)}{15(2J+1)}$
$[J, J-1, J-2, J-1]$	$\frac{2J(J-1)}{15(2J-1)}$	$\frac{-J(J-1)}{10(2J-1)}$	$\frac{J(J-1)}{15(2J-1)}$	$\frac{-J(J-1)}{10(2J-1)}$

### 2.5. Resonance-enhancement in FWM by continuum states

In the calculations of linestrengths for threefold-resonant FWM processes in the preceding sections well-defined sequences of angular momentum states  $[J_a, J_b, J_c, J_d]$  were postulated. In the case of resonance on bound states the frequencies at which they appear in the spectrum allow for a determination of the values of the angular momenta of the quantum states involved. In case of resonance enhancement on a dissociative state, related to a purely repulsive potential, or in the positive energy range of an attractive potential, this is not the case. Then all  $J$  values allowed by dipole transitions, connecting the continuum state to the FWM cycle, give rise to enhancement. Contributions of different  $J$  values interfere and must be summed coherently. The number of contributing  $J$  states in the continuum is at maximum three and at minimum one, depending on the  $\Omega$  values of the electronic states involved.

As an example we calculated the linestrengths in the threefold-resonant ground state CARS scheme of fig. 1 with the assumptions of  $\Omega_a = \Omega_b = \Omega_c = 0$  and the projected electronic angular momentum of the continuum state  $\Omega_d$  either 0 or  $\pm 1$ . In section 2.2 it was shown that in an isotropic medium two  $S$  factors play a role for this process:  $S_{0000}$  for the case of parallel linear polarizations and  $S_{10-10}$  for the case of crossed linear polarizations of the two incident beams. The Raman resonances give rise to a branching in conventional O( $J$ ), Q( $J$ ) and S( $J$ ) lines. The S and O lines may only be enhanced by an R respectively P transition on the first  $\omega_1$  resonance. For the Q lines there are two possibilities Q<sup>P</sup> and Q<sup>R</sup>, where the superscript denotes the angular momentum sequence of the first resonance. From the point of view of frequencies there is only one Q branch, but for the linestrengths a distinction has to be made between Q<sup>P</sup> and Q<sup>R</sup> lines because the resulting values are different. For the S and O lines there is only one possibility to complete the FWM cycle,  $[J, J+1, J+2, J+1]$  and  $[J, J-1, J-2, J-1]$  respectively. The linestrength factors are given in tables 3 and 4. For the Q lines the number of routes for completing the FWM cycle depends on the value of  $\Omega_d$  of the continuum. For  $\Omega_d = 0$  two channels and for  $\Omega_d = \pm 1$  three channels interfere respectively. For example the linestrength of the Q<sup>P</sup>( $J$ ) line, assuming  $\Omega_d = \pm 1$ , is determined by the coherent addition of the linestrength factors of the routes  $[J, J-1, J, J-1]$ ,  $[J, J-1, J, J+1]$  and  $[J, J-1, J, J]$  to be taken from table 4. By following this procedure the rotational linestrengths for the cases of linear parallel and linear crossed polarization for this ground-state resonant CARS process were calculated (see table 5).

Table 4  
Rotational line strength factors  $S_{jkm}^{000\pm 1}$  (eq. (8a)) for  $\Omega_a = \Omega_b = \Omega_c = 0$  and  $\Omega_d = 1$

	$S_{0000}^{000\pm 1}$	$S_{10-10}^{000\pm 1}$
$[J, J+1, J, J+1]$	$-\frac{(J+2)(5+8J+4J^2)}{30(2J+1)(2J+3)}$	$-\frac{J(J+2)(J+2)}{15(2J+1)(2J+3)}$
$[J, J+1, J, J-1]$	$-\frac{(J-1)(J+1)}{15(2J+1)}$	$\frac{(J-1)(J+1)}{20(2J+1)}$
$[J, J+1, J, J]$	$-\frac{(J+2)}{30}$	$-\frac{(J-3)}{60}$
$[J, J+1, J+2, J+1]$	$\frac{(J+1)(J+2)}{15(2J+3)}$	$-\frac{(J+1)(J+2)}{20(2J+3)}$
$[J, J-1, J, J-1]$	$-\frac{(4J^2+1)(J-1)}{30(2J-1)(2J+1)}$	$-\frac{(J-1)(J-1)(J+1)}{15(2J-1)(2J+1)}$
$[J, J-1, J, J+1]$	$-\frac{J(J+2)}{15(2J+1)}$	$\frac{J(J+2)}{20(2J+1)}$
$[J, J-1, J, J]$	$-\frac{(J-1)}{30}$	$-\frac{(J+4)}{60}$
$[J, J-1, J-2, J-1]$	$\frac{J(J-1)}{15(2J-1)}$	$-\frac{J(J-1)}{20(2J-1)}$

2.6. Polarization orientation of the wave generated in a FWM process

The elements of the third-order non-linear susceptibility tensor  $\chi^{(3)}$  and the related  $S$  factors are independent of the polarizations of the applied fields. The induced non-linear polarization  $P^{(3)}$  however does depend on the incident polarizations through eq. (2). The field of a monochromatic wave may be written as

$$E_\omega(t) = \frac{1}{2} [E_\omega(\cos \theta \hat{z} + \sin \theta e^{i\phi} \hat{x}) \exp(-i\omega t) + \text{c.c.}] . \tag{13}$$

A description of plane waves travelling along the  $\hat{y}$  axis is adopted and all spatial dependences are left out of the description at this point.  $\theta$  is the angle of the polarization vector relative to the  $\hat{z}$  axis. The factor  $e^{i\phi}$  is introduced to represent the different polarization states. For linearly polarized light  $\phi=0$  and  $\theta$  can have any value. For circularly polarized light  $\phi=\pi/2$  and  $\theta$  is either  $\pi/4$  (left) or  $3\pi/4$  (right).

Allowing for all possible polarizations in the  $xz$  plane the Cartesian components of the induced third-order non-linear polarization in eq. (2) can be rewritten as

$$P_z^{(3)}(\omega) = \{ \chi_{zzzz}^{(3)} \cos \theta_1 \cos \theta_2 \cos \theta_3 + \chi_{zzxx}^{(3)} \cos \theta_1 \sin \theta_2 \sin \theta_3 \exp[i(\phi_2 - \phi_3)] \\ + \chi_{zxzx}^{(3)} \sin \theta_1 \cos \theta_2 \sin \theta_3 \exp[i(\phi_1 - \phi_3)] + \chi_{zxxz}^{(3)} \sin \theta_1 \sin \theta_2 \cos \theta_3 \exp[i(\phi_1 - \phi_2)] \} E_{\omega_1} E_{\omega_2} E_{\omega_3} , \tag{14}$$

by using the expression for the fields of eq. (13). A similar expression can be derived for  $P_x^{(3)}(\omega)$ .

The polarization orientation of the generated wave is determined by the resultant of  $P_x^{(3)}$  and  $P_z^{(3)}$ . In case of resonance CARS, with production of a frequency  $\omega_{AS} = 2\omega_1 - \omega_2$  with linearly polarized incident waves, simple expressions follow. The pump frequency  $\omega_1$  may be chosen polarized along  $\hat{z}$  and the polarization of the Stokes wave  $\omega_2$  with an angle  $\theta_S$  with respect to  $\hat{z}$  without loss of generality. The polarization of the generated anti-Stokes wave is then given by

$$P^{(3)} = \chi_{xzzx}^{(3)} \sin \theta_S \hat{x} + \chi_{zzzz}^{(3)} \cos \theta_S \hat{z} . \tag{15}$$

It follows that the generated anti-Stokes has a polarization angle  $\theta_{AS}$  with respect to the  $\hat{z}$  axis given by

$$\theta_{AS} = \arctan \frac{P_x^{(3)}}{P_z^{(3)}} = \arctan \left( \frac{\chi_{xzzx}^{(3)}}{\chi_{zzzz}^{(3)}} \tan \theta_S \right). \quad (16)$$

The tensor elements  $\chi_{xzzx}^{(3)}$  and  $\chi_{zzzz}^{(3)}$  both depend on linestrength factors  $S$  that are different for particular FWM processes or  $J$  states probed. As a consequence we find that in general the polarization orientation of the anti-Stokes wave will vary throughout the CARS spectrum. In the two simplest cases this is, however, not true. When both the  $\omega_1$  and  $\omega_2$  waves are linearly and parallelly polarized, only  $\chi_{zzzz}^{(3)}$  is needed and the anti-Stokes wave is also linearly polarized parallel to the incident waves, independent of any resonance. In case of crossed linear polarizations only  $\chi_{xzzx}^{(3)}$  is appropriate and we find that the anti-Stokes wave is polarized parallel to the Stokes wave throughout the CARS spectrum.

Finally we consider the effect of a polarization analyzer, again under the condition of linearly polarized beams  $\omega_1$  and  $\omega_2$ , with  $\omega_1$  chosen along  $\hat{z}$  and  $\omega_2$  with an angle  $\theta_S$  with respect to  $\hat{z}$ . This configuration is depicted in fig. 3. When the axis of the analyzer  $e_T$  is set at angle  $\theta_T$  (with respect to  $\hat{z}$ ) we find

$$P^{(3)} \cdot e_T = P_x^{(3)} \sin \theta_T + P_z^{(3)} \cos \theta_T = \chi_{xzzx}^{(3)} \sin \theta_S \sin \theta_T + \chi_{zzzz}^{(3)} \cos \theta_S \cos \theta_T. \quad (17)$$

The total intensity (without analyzer) becomes

$$I_{CARS} \propto |P^{(3)}|^2 = |\chi_{xzzx}^{(3)} \sin \theta_S|^2 + |\chi_{zzzz}^{(3)} \cos \theta_S|^2, \quad (18)$$

and with analyzer

$$I_{CARS} \propto |P^{(3)} \cdot e_T|^2 = |\chi_{xzzx}^{(3)} \sin \theta_S \sin \theta_T + \chi_{zzzz}^{(3)} \cos \theta_S \cos \theta_T|^2. \quad (19)$$

### 3. Applications in resonance CARS

Resonance CARS measurements were performed in  $I_2$  and  $Br_2$  vapours. A pump beam, from a fixed-frequency ( $\omega_1$ ) narrow-band Nd-YAG laser at 532 nm colinearly propagates with a wavelength-tunable Stokes beam ( $\omega_2$ ) along a chosen  $\hat{y}$  axis. The beams are focused in a gas cell containing the non-linear medium. Either the total intensity or the intensity transmitted through a polarization analyzer of the generated wave at  $\omega_{AS} = 2\omega_1 - \omega_2$  is detected (see fig. 3). In previous papers the frequency dependence of resonance CARS in  $I_2$  [13] and  $Br_2$  [17] was discussed. Well-known characteristics of threefold-resonant CARS spectra are the appearance of selected rotational lines in series of vibrational overtones. It suffices to note that a precise determination of resonance frequencies allows for an unambiguous assignment of the CARS spectral features in sequences of  $J$  states. In  $Br_2$  only a single FWM process could be observed, namely a ground-state resonant CARS process enhanced by bound transitions in the  $B^3\Pi_{u0}^+ - X^1\Sigma_g^+$  system and by a continuum state at the one-photon level. In  $I_2$ , apart from a similar ground-state resonant CARS process, also two distinguishable excited-state CARS processes were identified (fig. 1) in which a continuum state at the two-photon level gives rise to resonance enhancement. In the following we will demonstrate how to invoke the theoretical framework on rotational linestrengths devel-

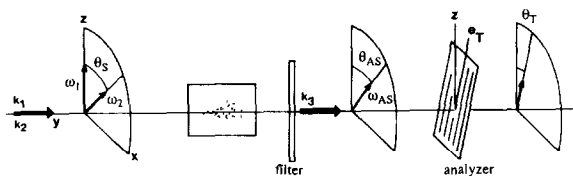


Fig. 3. Collinear setup for resonant CARS measurements; the analyzer is an option that was not used in measurements of total intensities; focusing lenses are not shown.

Table 5  
Linestrengths for ground-state resonant CARS <sup>a)</sup>

	Parallel ( $\Omega_d=0$ )	Parallel ( $\Omega_d=\pm 1$ )	Crossed ( $\Omega_d=0$ )	Crossed ( $\Omega_d=\pm 1$ )
Q <sup>R</sup> lines	$\frac{(J+1)(4J+5)}{15(2J+3)}$	$\frac{-(3J+5)(J+1)}{15(2J+3)}$	$\frac{-J(J+1)}{30(2J+3)}$	$\frac{-J(J+1)}{60(2J+3)}$
S <sup>R</sup> lines	$\frac{2(J+1)(J+2)}{15(2J+3)}$	$\frac{(J+1)(J+2)}{15(2J+3)}$	$\frac{-(J+1)(J+2)}{10(2J+3)}$	$\frac{-(J+1)(J+2)}{20(2J+3)}$
Q <sup>P</sup> lines	$\frac{J(4J-1)}{15(2J-1)}$	$\frac{-J(3J-2)}{15(2J-1)}$	$\frac{-J(J+1)}{30(2J-1)}$	$\frac{-J(J+1)}{60(2J-1)}$
O <sup>P</sup> lines	$\frac{2J(J-1)}{15(2J-1)}$	$\frac{J(J-1)}{15(2J-1)}$	$\frac{-J(J-1)}{10(2J-1)}$	$\frac{-J(J-1)}{20(2J-1)}$

<sup>a)</sup> We note here that in a preliminary report on resonance CARS in Br<sub>2</sub> molecules [17] the linestrengths for Q<sup>R</sup> lines (parallel polarization) and Q<sup>P</sup> lines (crossed polarization), both in case  $\Omega_d=0$ , were erroneously interchanged.

oped in section 2 for a comparison with the signal intensities observed in the various processes.

### 3.1. Polarization-dependent intensity ratios

Given a certain polarization configuration first the appropriate  $\chi^{(3)}$  elements must be determined. Assuming linear polarizations for the incident waves it is shown in eq. (18) that the CARS intensity in general has a parallel contribution proportional to  $\chi_{zzzz}^{(3)}$  and a crossed contribution given by  $\chi_{xzzx}^{(3)}$ . For all resonance schemes the  $\chi_{zzzz}^{(3)}$  element corresponds to the  $S_{0000}$ -rotational linestrength factor, whereas for the  $\chi_{xzzx}^{(3)}$  element it is process dependent. In eq. (10) the transformation of  $\chi_{xzzx}^{(3)}$  is given for the ground-state resonant CARS process and the transformation for the other processes can be worked out in an analogous way. It follows that e.g. the rotational linestrength in case of crossed polarizations of the incident beams in the ground-state resonant CARS process is determined by  $S_{10-10}$ , while  $S_{1-100}$  is needed in the excited-state CARS processes. The corresponding reduced linestrength factors  $s_{10-10}$  and  $s_{1-100}$  can be extracted from table 1. At this point the assumption of an isotropic medium is made.

Next we have to determine the molecular prefactors  $\Omega^{abcd}$  that depend on the molecular system involved. In the I<sub>2</sub> and Br<sub>2</sub> experiments the CARS processes are resonantly-enhanced by bound transitions in the B<sup>3</sup>Π<sub>u0</sub><sup>+</sup>-X<sup>1</sup>Σ<sub>g</sub><sup>+</sup> system, thus involving  $\Omega=0$  states. Continuum enhancement in ground-state CARS is achieved at the one-photon level by B<sup>3</sup>Π<sub>u0</sub><sup>+</sup> ( $\Omega=0$ ) and <sup>1</sup>Π<sub>1u</sub> ( $\Omega=\pm 1$ ). Their contribution depends on the different overlap integrals and the electronic transition moments of eq. (7). For the excited-state CARS processes in I<sub>2</sub>, however, continuum enhancement is obtained at the two-photon level where an  $\Omega_c=0$  repulsive state is assumed [9]. In table 2 the different molecular prefactors needed in various cases are given.

For a specified [ $J_a, J_b, J_c, J_d$ ] combination the appropriate  $\Omega^{abcd}$  and  $s_{jklm}$  factors must be multiplied next. For the case of  $\Omega^{0000}$  the resulting rotational linestrengths are given in table 3. As explained in section (2.5) resonance-enhancement by a continuum can be taken into account in the rotational linestrength by coherently adding all allowed  $J$ -routes. In the case of ground-state resonant CARS this means a summation over  $J_d$  states, whereas a summation over  $J_c$  states has to be evaluated for the excited-state CARS processes. So finally all allowed  $J$ -combinations, determined by molecular prefactors, must be added. In tables 5 and 6 the rotational linestrengths are tabulated for the cases of  $\Omega=0$  or 1 and for parallel and crossed polarizations. These values must be squared to compare with observed CARS rotational linestrengths.

The calculated  $J$ -dependence of the intensity ratios (obtained from table 6) of the characteristic doublets [9,13] in the non-parametric excited-state CARS process ( $\Omega_c=0$ ) for parallel and crossed polarization is shown

Table 6  
Linestrengths for excited-state resonant CARS

	Parallel ( $\Omega_c=0$ )	Parallel ( $\Omega_c=\pm 1$ )	Crossed ( $\Omega_c=0$ )	Crossed ( $\Omega_c=\pm 1$ )
Q <sup>R</sup> lines	$\frac{(J+1)(4J+3)}{15(2J+1)}$	$-\frac{(J+1)(3J+1)}{15(2J+1)}$	$-\frac{(J+1)(J+2)}{30(2J+1)}$	$-\frac{(J+1)(J+2)}{60(2J+1)}$
O <sup>R</sup> lines	$\frac{2J(J+1)}{15(2J+1)}$	$\frac{J(J+1)}{15(2J+1)}$	$-\frac{J(J+1)}{10(2J+1)}$	$-\frac{J(J+1)}{20(2J+1)}$
Q <sup>P</sup> lines	$\frac{J(4J+1)}{15(2J+1)}$	$-\frac{J(3J+2)}{15(2J+1)}$	$-\frac{J(J-1)}{30(2J+1)}$	$-\frac{J(J-1)}{60(2J+1)}$
S <sup>P</sup> lines	$\frac{2J(J+1)}{15(2J+1)}$	$\frac{J(J+1)}{15(2J+1)}$	$-\frac{J(J+1)}{10(2J+1)}$	$-\frac{J(J+1)}{20(2J+1)}$

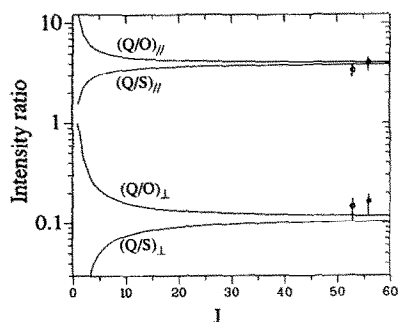


Fig. 4. Theoretical  $J$ -dependence of intensity ratios for parallel (upper) and crossed (lower) polarization for the excited-state parametric CARS process as discussed in the text. Experimental points for  $I_2$  are given. Black circles (●) denote the linestrength ratio  $Q/O$  and open circles (○) ratio of  $Q/S$  lines. In the estimated uncertainties in the data points the uncertainty in the relative angles between polarization vectors are included.

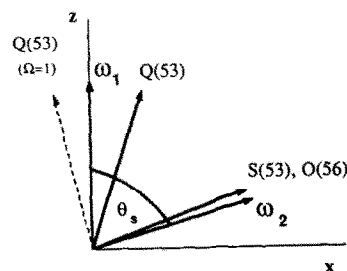


Fig. 5. Polarization configuration for excited-state CARS experiment. The pump  $\omega_1$  is linearly polarized along the  $z$  axis, while the linearly polarized Stokes wave makes an angle of  $\theta_s=70^\circ$  with the  $z$  axis. Calculated angles  $\theta_{AS}$  are shown for Q and O/S branches in case of a continuum state with  $\Omega_c=0$  (black arrow) as well as  $\pm 1$  (dashed arrow).

in fig. 4. A few experimental points for  $I_2$  are inserted as well and agreement with theoretical prediction is obtained.

### 3.2. Polarization of the anti-Stokes wave in excited-state parametric CARS

In the setup with a polarization analyzer (see fig. 3) the excited-state parametric CARS process in  $I_2$  was investigated in the energy range with a Stokes shift of 910–925  $\text{cm}^{-1}$ . The angle between the linear polarization vectors of the incident waves was chosen at  $\theta_s=70^\circ$ . The polarization configuration of the waves involved is represented in fig. 5. Applying eqs. (15) and (16), inserting the appropriate linestrength factors (from table 6) pertaining to the two relevant tensor elements  $\chi_{zzx}^{(3)}$  and  $\chi_{zzz}^{(3)}$ , the polarization orientation of the generated wave was calculated. Angles  $\theta_{AS}$  of  $19^\circ$  for the Q<sup>P</sup>(53) and Q<sup>R</sup>(56) and  $64^\circ$  for the O(56) and S(53) lines were deduced. To verify these drastic polarization effects CARS spectra of these four resonances were recorded at different settings  $\theta_T$  of the polarization analyzer. These spectra are shown in fig. 6. Indeed it is found that for  $\theta_T$  at a value perpendicular to the calculated values for  $\theta_{AS}$  the signals in the Q branch (at  $\theta_T=-70^\circ$ ) or the O/S branch (at  $\theta_T=-25^\circ$ ) vanish. The upper spectrum in fig. 6 is taken at  $\theta_T=60^\circ$  for which doublet ratios of 0.5

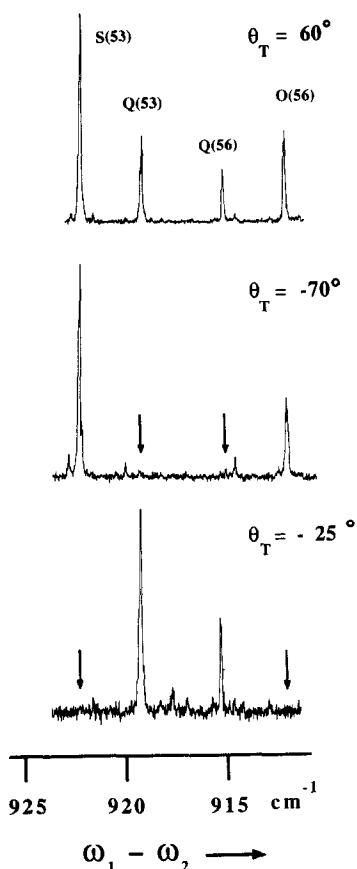


Fig. 6. Excited-state parametric CARS spectra taken with different analyser settings ( $\theta_T$  with respect to the  $\hat{z}$  axis) and an angle of  $\theta_S = 70^\circ$  between the two incoming linearly polarized beams.

and 0.45 are predicted for the Q/O(56) and Q/S(53) lines respectively. This agrees well with the observed ratios of 0.6 and 0.43.

So we conclude that the theory for calculating the orientation of the polarization vector of the anti-Stokes wave produces excellent agreement with the features observed in  $I_2$ . These calculations were based on the assumption that the continuum state at the two-photon level is an  $\Omega_c = 0$  state. To verify this assumption  $\theta_{AS}$  was also calculated for an  $\Omega_c = 1$  continuum state. Again the lines of the O and S branch show a maximum intensity near  $\theta_{AS} = 64^\circ$ , but the lines of the Q branch near  $\theta_{AS} = -14^\circ$  for  $J$  values 53 and 56. This is shown in fig. 5. The strong dependence of the polarization orientation of the generated CARS wave on  $\Omega_c$  is another tool to determine the electronic character of states involved in the resonant CARS processes. The assumption of enhancement by a  $0_g^+$ -continuum state in  $I_2$  [13] is supported by the present polarization data.

#### 4. Concluding remarks

Although the formalism presented in this paper can be applied quite generally, several assumptions are made. E.g. it is implicitly assumed that a generated wave propagates in the direction determined by a phase-matching condition. Furthermore the effects of fast relaxation mechanisms are ignored and calculations hold for the stationary limit. Also effects of saturation are not included as the expression for  $\chi^{(3)}$  is deduced from a perturbative

approach and higher-order  $\chi^{(n)}$  terms are left out. Within these restrictions the analytical expressions for the rotational linestrengths are applicable for diatomics and symmetric-top molecules in isotropic gaseous media. Furthermore they may be used for any threefold resonant FWM process including e.g. the case of resonance-enhanced third harmonic generation. Particularly an application in the new powerful technique of degenerate four-wave mixing, that is now finding widespread use in combustion diagnostics, should follow straightforwardly. It should be noted however that extreme care must be taken to select the appropriate terms of the  $\chi^{(3)}$  tensor for this DFWM process. Work along these lines is in progress.

## References

- [1] A.C. Eckbreth, *Combustion Flame* 39 (1980) 133.
- [2] R.J. Hall, *Combustion Flame* 35 (1979) 47.
- [3] B. Attal-Tretout and P. Bouchardy, *Rech. Aerosp.* 5 (1987) 19.
- [4] P. Ewart and S.V. O'Leary, *Opt. Letters* 11 (1986) 279.
- [5] T. Dreier and D.J. Rakestraw, *Appl. Phys. B* 50 (1990) 479.
- [6] H. Bervas, B. Attal-Tretout, S. Le Boiteux and J.-P. Taran, *J. Phys. B* 25 (1992) 949.
- [7] R.L. Abrams and R.C. Lind, *Opt. Letters* 2 (1978) 94; 3 (1978) 205 (E).
- [8] B. Attal-Tretout, P. Monot and K. Muller-Dethlefs, *Mol. Phys.* 73 (1991) 1257.
- [9] I. Aben, W. Ubachs, G. van der Zwan and W. Hogervorst, *Mol. Phys.* 76 (1992) 591.
- [10] Y.R. Shen, *The principles of nonlinear optics* (Wiley, New York, 1984).
- [11] D.C. Hanna, M.A. Yuratich and D. Cotter, *Springer series in optical sciences*, Vol. 17. *Nonlinear optics of free atoms and molecules* (Springer, Berlin, 1979).
- [12] Y. Prior, *IEEE J. Quantum Electron.* QE-20 (1984) 37.
- [13] I. Aben, W. Ubachs, P. Levelt, G. van der Zwan and W. Hogervorst, *Phys. Rev. A* 44 (1991) 5881.
- [14] R.N. Zare, *Angular momentum* (Wiley, New York, 1988).
- [15] P.N. Butcher and D. Cotter, *The elements of nonlinear optics* (Cambridge Univ. Press, Cambridge, 1990).
- [16] D.A. Kleinman, *Phys. Rev.* 126 (1962) 1977.
- [17] I. Aben, W. Ubachs, G. van der Zwan and W. Hogervorst, *Chem. Phys. Letters* 198 (1992) 149.